

A novel setup for femtosecond pump-repump-probe IR spectroscopy with few cycle CEP stable pulses

Maximilian Bradler,² Jasper C. Werhahn,¹ Daniel Hutzler,¹ Simon Fuhrmann,¹ Rupert Heider,¹ Eberhard Riedle,^{2,*} Hristo Iglev,¹ and Reinhard Kienberger¹

¹Physik-Department E11, Technische Universität München, James-Frank-Str. 1, 85748 Garching, Germany

²Lehrstuhl für BioMolekulare Optik, Ludwig-Maximilians-Universität, Oettingenstr. 67, 80538 Munich, Germany

*Eberhard.Riedle@Physik.uni-muenchen.de

Abstract: We present a three-color mid-IR setup for vibrational pump-repump-probe experiments with a temporal resolution well below 100 fs and a freely selectable spectral resolution of 20 to 360 cm^{-1} for the pump and repump. The usable probe range without optical realignment is 900 cm^{-1} . The experimental design employed is greatly simplified compared to the widely used setups, highly robust and includes a novel means for generation of tunable few-cycle pulses with stable carrier-envelope phase. A Ti:sapphire pump system operating with 1 kHz and a modest 150 fs pulse duration supplies the total pump energy of just 0.6 mJ. The good signal-to-noise ratio of the setup allows the determination of spectrally resolved transient probe changes smaller than $6 \cdot 10^{-5}$ OD at 130 time delays in just 45 minutes. The performance of the spectrometer is demonstrated with transient IR spectra and decay curves of HDO molecules in lithium nitrate trihydrate and ice and a first all MIR pump-repump-probe measurement.

© 2013 Optical Society of America

OCIS codes: (300.6190) Spectrometers; (300.6340) Spectroscopy, infrared; (300.6500) Spectroscopy, time-resolved; (300.6530) Spectroscopy, ultrafast; (320.7110) Ultrafast nonlinear optics; (320.7150) Ultrafast spectroscopy.

References and links

1. H. Graener, G. Seifert, and A. Laubereau, "New spectroscopy of water using tunable picosecond pulses in the infrared," *Phys. Rev. Lett.* **66**(16), 2092–2095 (1991).
2. S. Woutersen, U. Emmerichs, and H. J. Bakker, "Femtosecond mid-IR pump-probe spectroscopy of liquid water: evidence for a two-component structure," *Science* **278**(5338), 658–660 (1997).
3. M. T. Zanni and R. M. Hochstrasser, "Two-dimensional infrared spectroscopy: a promising new method for the time resolution of structures," *Curr. Opin. Struct. Biol.* **11**(5), 516–522 (2001).
4. M. Khalil, N. Demirdöven, and A. Tokmakoff, "Coherent 2D IR spectroscopy: molecular structure and dynamics in solution," *J. Phys. Chem. A* **107**(27), 5258–5279 (2003).
5. E. T. J. Nibbering and T. Elsaesser, "Ultrafast vibrational dynamics of hydrogen bonds in the condensed phase," *Chem. Rev.* **104**(4), 1887–1914 (2004).
6. D. Kraemer, M. L. Cowan, A. Paarmann, N. Huse, E. T. J. Nibbering, T. Elsaesser, and R. J. D. Miller, "Temperature dependence of the two-dimensional infrared spectrum of liquid H_2O ," *Proc. Natl. Acad. Sci. U.S.A.* **105**(2), 437–442 (2008).
7. H. J. Bakker and J. L. Skinner, "Vibrational spectroscopy as a probe of structure and dynamics in liquid water," *Chem. Rev.* **110**(3), 1498–1517 (2010).
8. J. C. Werhahn, S. Pandelov, S. S. Xantheas, and H. Iglev, "Dynamics of weak, bifurcated, and strong hydrogen bonds in lithium nitrate trihydrate," *J. Phys. Chem. Lett.* **2**(13), 1633–1638 (2011).
9. P. Hamm, S. Wiemann, M. Zurek, and W. Zinth, "Highly sensitive multichannel spectrometer for subpicosecond spectroscopy in the midinfrared," *Opt. Lett.* **19**(20), 1642–1644 (1994).
10. J. L. Bingham, C. L. Kohnhorst, G. A. Van Meter, B. A. McElroy, E. A. Rakowski, B. W. Caplins, T. A. Gutowski, C. J. Stromberg, C. E. Webster, and E. J. Heilweil, "Time-resolved vibrational spectroscopy of [FeFe]-hydrogenase model compounds," *J. Phys. Chem. A* **116**(27), 7261–7271 (2012).

11. P. M. Donaldson, H. Strzalka, and P. Hamm, "High sensitivity transient infrared spectroscopy: a UV/visible transient grating spectrometer with a heterodyne detected infrared probe," *Opt. Express* **20**(12), 12761–12770 (2012).
12. R. A. Kaindl, M. Wurm, K. Reimann, P. Hamm, A. W. Weiner, and M. Woerner, "Generation, shaping, and characterization of intense femtosecond pulses tunable from 3 to 20 μm ," *J. Opt. Soc. Am. B* **17**(12), 2086–2094 (2000).
13. N. Demirdöven, M. Khalil, O. Golonzka, and A. Tokmakoff, "Dispersion compensation with optical materials for compression of intense sub-100-fs mid-infrared pulses," *Opt. Lett.* **27**(6), 433–435 (2002).
14. J. B. Asbury, T. Steinel, and M. D. Fayer, "Vibrational echo correlation spectroscopy probes of hydrogen bond dynamics in water and methanol," *J. Lumin.* **107**(1-4), 271–286 (2004).
15. H. S. Chung, M. Khalil, A. W. Smith, and A. Tokmakoff, "Transient two-dimensional IR spectrometer for probing nanosecond temperature-jump kinetics," *Rev. Sci. Instrum.* **78**(6), 063101 (2007).
16. S. Park, K. Kwak, and M. D. Fayer, "Ultrafast 2D-IR vibrational echo spectroscopy: a probe of molecular dynamics," *Laser Phys. Lett.* **4**(10), 704–718 (2007).
17. S. H. Shim and M. T. Zanni, "How to turn your pump-probe instrument into a multidimensional spectrometer: 2D IR and Vis spectroscopies via pulse shaping," *Phys. Chem. Chem. Phys.* **11**(5), 748–761 (2009).
18. K. C. Jones, Z. Ganim, C. S. Peng, and A. Tokmakoff, "Transient two-dimensional spectroscopy with linear absorption corrections applied to temperature-jump two-dimensional infrared," *J. Opt. Soc. Am. B* **29**(1), 118–129 (2012).
19. D. R. Skoff, J. E. Laaser, S. S. Mukherjee, C. T. Middleton, and M. T. Zanni, "Simplified and economical 2D IR spectrometer design using a dual acousto-optic modulator," *Chem. Phys.* in press., doi:10.1016/j.chemphys.2012.08.019.
20. D. Eisenberg and W. Kauzmann, *The Structure and Properties of Water* (Oxford University, 1969).
21. F. Franks, *Water: A Comprehensive Treatise* (Plenum Press, 1972).
22. Y. Tanimura and S. Mukamel, "2-dimensional femtosecond vibrational spectroscopy of liquids," *J. Chem. Phys.* **99**(12), 9496–9511 (1993).
23. M. Bradler, C. Homann, and E. Riedle, "Mid-IR femtosecond pulse generation on the microjoule level up to 5 μm at high repetition rates," *Opt. Lett.* **36**(21), 4212–4214 (2011).
24. M. Bradler, P. Baum, and E. Riedle, "Femtosecond continuum generation in bulk laser host materials with sub- μJ pump pulses," *Appl. Phys. B* **97**(3), 561–574 (2009).
25. J. Piel, M. Beutter, and E. Riedle, "20-50-fs pulses tunable across the near infrared from a blue-pumped noncollinear parametric amplifier," *Opt. Lett.* **25**(3), 180–182 (2000).
26. I. Hartl and W. Zinth, "A novel spectrometer system for the investigation of vibrational energy relaxation with sub-picosecond time resolution," *Opt. Commun.* **160**(1–3), 184–190 (1999).
27. V. Petrov, F. Rotermund, and F. Noack, "Generation of high-power femtosecond light pulses at 1 kHz in the mid-infrared spectral range between 3 and 12 μm by second-order nonlinear processes in optical crystals," *J. Opt. A, Pure Appl. Opt.* **3**(3), R1–R19 (2001).
28. D. Brida, C. Manzoni, G. Cirri, M. Marangoni, S. De Silvestri, and G. Cerullo, "Generation of broadband mid-infrared pulses from an optical parametric amplifier," *Opt. Express* **15**(23), 15035–15040 (2007).
29. W. E. White, F. G. Patterson, R. L. Combs, D. F. Price, and R. L. Shepherd, "Compensation of higher-order frequency-dependent phase terms in chirped-pulse amplification systems," *Opt. Lett.* **18**(16), 1343–1345 (1993).
30. R. Trebino, K. W. De Long, D. N. Fittinghoff, J. N. Sweetser, M. A. Krumbügel, B. A. Richman, and D. J. Kane, "Measuring ultrashort laser pulses in the time-frequency domain using frequency-resolved gating," *Rev. Sci. Instrum.* **68**(9), 3277–3295 (1997).
31. A. Baltuska, M. Überacker, E. Goulielmakis, R. Kienberger, V. S. Yakovlev, T. Udem, T. W. Hänsch, and F. Krausz, "Phase-controlled amplification of few-cycle laser pulses," *IEEE J. Sel. Top. Quantum Electron.* **9**(4), 972–989 (2003).
32. G. Cerullo, A. Baltuska, O. D. Mücke, and C. Vozzi, "Few-optical-cycle light pulses with passive carrier-envelope phase stabilization," *Laser Photonics Rev.* **5**(3), 323–351 (2011).
33. S. Pandalov, B. M. Pilles, J. C. Werhahn, and H. Iglev, "Time-resolved dynamics of the OH stretching vibration in aqueous NaCl hydrate," *J. Phys. Chem. A* **113**(38), 10184–10188 (2009).
34. H. Graener, G. Seifert, and A. Laubereau, "Vibrational and reorientational dynamics of water molecules in liquid matrices," *Chem. Phys.* **175**(1), 193–204 (1993).
35. H. J. Bakker, J. J. Giljames, and A. J. Lock, "Energy transfer in single hydrogen-bonded water molecules," *ChemPhysChem* **6**(6), 1146–1156 (2005).
36. S. Woutersen, U. Emmerichs, H. K. Nienhuys, and H. J. Bakker, "Anomalous temperature dependence of vibrational lifetimes in water and ice," *Phys. Rev. Lett.* **81**(5), 1106–1109 (1998).
37. H. Iglev, M. Schmeisser, K. Simeonidis, A. Thaller, and A. Laubereau, "Ultrafast superheating and melting of bulk ice," *Nature* **439**(7073), 183–186 (2006).
38. C. Schriefer, S. Lochbrunner, E. Riedle, and D. J. Nesbitt, "Ultrasensitive ultraviolet-visible 20 fs absorption spectroscopy of low vapor pressure molecules in the gas phase," *Rev. Sci. Instrum.* **79**(1), 013107 (2008).
39. U. Megerle, I. Pugliesi, C. Schriefer, C. F. Sailer, and E. Riedle, "Sub-50 fs broadband absorption spectroscopy with tunable excitation: Putting the analysis of ultrafast molecular dynamics on solid ground," *Appl. Phys. B* **96**(2-3), 215–231 (2009).

40. M. S. Lynch, K. M. Slenkamp, M. Cheng, and M. Khalil, "Coherent fifth-order visible-infrared spectroscopies: ultrafast nonequilibrium vibrational dynamics in solution," *J. Phys. Chem. A* **116**(26), 7023–7032 (2012).
 41. M. L. Groot, L. J. G. W. van Wilderen, and M. Di Donato, "Time-resolved methods in biophysics. 5. Femtosecond time-resolved and dispersed infrared spectroscopy on proteins," *Photochem. Photobiol. Sci.* **6**(5), 501–507 (2007).
 42. P. Hamm, R. A. Kaindl, and J. Stenger, "Noise suppression in femtosecond mid-infrared light sources," *Opt. Lett.* **25**(24), 1798–1800 (2000).
 43. Y. Deng, A. Schwarz, H. Fattahi, M. Ueffing, X. Gu, M. Ossiander, T. Metzger, V. Pervak, H. Ishizuki, T. Taira, T. Kobayashi, G. Marcus, F. Krausz, R. Kienberger, and N. Karpowicz, "Carrier-envelope-phase-stable, 1.2 mJ, 1.5 cycle laser pulses at 2.1 μm ," *Opt. Lett.* **37**(23), 4973–4975 (2012).
-

1. Introduction

Infrared pump-probe and two dimensional spectroscopy are very powerful tools to elucidate the complex ultrafast dynamics of an abundance of condensed systems [1–4]. For hydrogen bonded systems, high-lying stretching vibrations of the hydrogen bond donors can be utilized as local probe of the chemical environment of the donor group [1,5–8]. Despite the fact, that ultrafast infrared pump probe spectroscopy is used in many different disciplines including biology and chemistry, detailed descriptions of the setups remain scarce [5,9–11]. Modern developments in two dimensional IR spectroscopy and photon echo techniques are much better documented [12–19]. The intention of this paper is to demonstrate new sources of femtosecond pulses with a greatly simplified concept and a wide variability of output parameters. They are combined to a new three-color spectrometer with very flexible operating parameters. We include detailed insight into the construction of the spectrometer, which we hope will prove useful particularly for newcomers to the field.

With the advent of ever shorter laser pulses, the time resolution of pump-probe setups evolved from several picoseconds down into the 100 fs regime, allowing the resolution of increasingly fast dynamics. Important information on the chemical nature of the vicinity of the probed molecule lies in the spectral position of the vibration under consideration. It is for example commonly agreed on, that an increased red shift in the position of an OH stretching vibration correlates with an increased strength of the corresponding hydrogen bond [20,21]. This means that complementary information can be obtained with long pulses with a narrow spectrum, as compared to the information gained from investigations with extremely short pulses that lack high spectral resolution. More advanced techniques like photon echo spectroscopy partially circumvent this problem, but the interpretation of the obtained data is quite demanding and has to rely heavily on simulations, where the physical result depends on the applied theoretical model [6,22]. Pump-probe spectroscopy still yields the most quantitative and direct information.

With pump-repump-probe spectroscopy, higher lying vibrational levels can be reached via successive excitation. These high-lying states are a very convenient probe of the shape of the potential of the hydrogen bond under consideration. Experimental data on the shape of the H bond potential in different chemical environments are in turn very valuable information for theory to accomplish a better modeling of this still poorly understood interaction. It could furthermore open a pathway towards optically induced chemical reactions like proton transfer, which has not yet been achieved with infrared pulses.

We present first results obtained with a newly developed optical setup that allows mid-IR pump-repump-probe spectroscopy with a time resolution significantly shorter than 100 fs. The infrared pulses are generated via a recently demonstrated hybrid NOPA layout [23]. In order to achieve a selective excitation of the vibrational modes under investigation, the pump pulses are tunable in the range from 2,000 to 10,000 cm^{-1} , and their spectral widths are controlled by a spectral grating selector. The pulses generated in this way have a spectral bandwidth between 20 and 360 cm^{-1} and pulse durations between 50 and 850 fs, with typical pulse energies of 3 μJ . The probe pulses are shorter than 50 fs (FWHM up to 450 cm^{-1}), yielding few-cycle mid-IR pulses with unprecedented spectral width. The Fourier limit for these pulses is below 30 fs.

This paper is organized as follows: In Section 2 we will present the experimental setup and briefly discuss the layout of the used optical parametric amplifiers and grating selectors. Section 3 presents a full characterization of the employed pulses, including their spectral and temporal phase and we will demonstrate that all our pulses have a stable carrier envelope phase (CEP). Section 4 shows first measurements with the new setup, where we significantly improve recently published measurements on OH stretching vibration lifetimes of HDO molecules in lithium nitrate trihydrate [8]. Section 5 concludes with a detailed classification and comparison to existing state of the art spectrometers.

2. Experimental setup

The basic layout of our setup is illustrated in Fig. 1(a). As source we use a Ti:sapphire based laser system (CPA 2010; Clark MXR) which delivers 779 nm pulses at 1 kHz repetition rate with a pulse duration of 150 fs and a pulse energy of 900 μJ . For the current setup we use 600 μJ . The remaining pulse energy is used for diagnostics and further experiments.

To generate the infrared pump pulses we use a hybrid pumping technique [23] which allows the generation of femtosecond pulses tunable from 1 to over 5 μm at the μJ level. The idea of the amplifier is shown in Fig. 1(b). A near-infrared continuum is generated in a 4 mm YAG plate (SCG) [24] and amplified in a noncollinear optical parametric amplifier (pre-NOPA) pumped by 60 μJ of the second harmonic of the laser light [25]. As amplifier crystal we use a 2 mm thick BBO crystal (type I, 32° cutting angle). Pulses on the μJ level which are tunable between 900 nm and 1.6 μm are generated in this pre-amplifier. Here, the noncollinearity is only used to geometrically separate the pump and idler pulses. In this work we denominate the light which is amplified with the term “signal light”, and with the term “idler light” the light which is newly generated, independent from their wavelengths.

The near-infrared pulses are then further amplified in a collinear amplifier (IR-OPA) pumped by the 120 μJ of the fundamental laser light left over in the second harmonic generation (SHG). Here we use a 1.5 mm thick LiNbO₃ crystal (type I, cut at 45°) as amplifier material. The idler pulses which are produced during this amplification process spectrally range between 1.6 to 5.0 μm (2,000 to 6,250 cm^{-1}) and typically have pulse energies of several μJ . The full details and advantages of this concept have been presented recently [23]. The blue pumped pre-amplification drastically increases the MIR output energy especially at the spectral limits of the main amplifier. The high output can be reached with moderate pump intensities in the IR-OPA that allow the use of nonlinear crystals like LiIO₃ which were previously considered critical for fs OPA-operation due to the low damage threshold [26–28]. The amplifier is operated completely collinear to avoid any spatial chirp of the idler pulses. A good method to experimentally realize the collinearity is to minimize the spatial separation between signal and pump light. Since the pump, signal, and idler pulses propagate in the same direction dichroic optics are used to separate the 779 nm light (HR 800 nm, HT 1 - 5 μm) and filters (germanium or silicon plates) to separate the signal pulses. Due to the high refractive index of germanium and silicon an anti-reflection coating is needed. It should be mentioned that germanium plates have a drastically decreased infrared transmission if they are illuminated by high intensity 800 nm light and therefore these filters should be placed in the unfocussed beams or after the separation of the 800 nm light. If the signal pulses are intended to be used for the experiment to cover the range from 1.0 to 1.6 μm (6,250 - 10,000 cm^{-1}) a slight noncollinearity in the IR-OPA already leads to spatial separation from the pump and idler pulses and for the signal pulses no spatial chirp will occur. For all measurements shown in this paper we use the idler pulses and all IR-OPAs are operated in the collinear geometry.

In some experiments an energetically selective excitation of the sample is required. A spectral selector [29] whose setup is shown in Fig. 1(d) allows decreasing the spectral bandwidth of the pump pulses down to 20 cm^{-1} . A gold coated grating (3 cm x 3 cm, Horiba Scientific GmbH) with a blaze wavelength of 3 μm and 100 lines/mm disperses the infrared light. A $f = 100$ mm calcium fluoride (CaF₂) lens is used to focus the light onto the end mirror

which reflects the light back to the entrance of the selector. By changing the width of the slit in front of the end mirror the spectral width of the pump pulses can be adjusted continuously down to 20 cm^{-1} . To separate the input and output pulses at the exit of the selector a slight vertical shift is introduced by the end mirror. To maintain collimation for the transverse plane of the pump pulses at the exit and zero dispersion, the distance between lens and grating must be equal to the focal length [29]. For the sagittal plane the distance between lens and end mirror must be the focal length. The energy of the pump pulses also decreases proportionally to the narrower bandwidth. The throughput of the selector is around 85% for the full bandwidth.

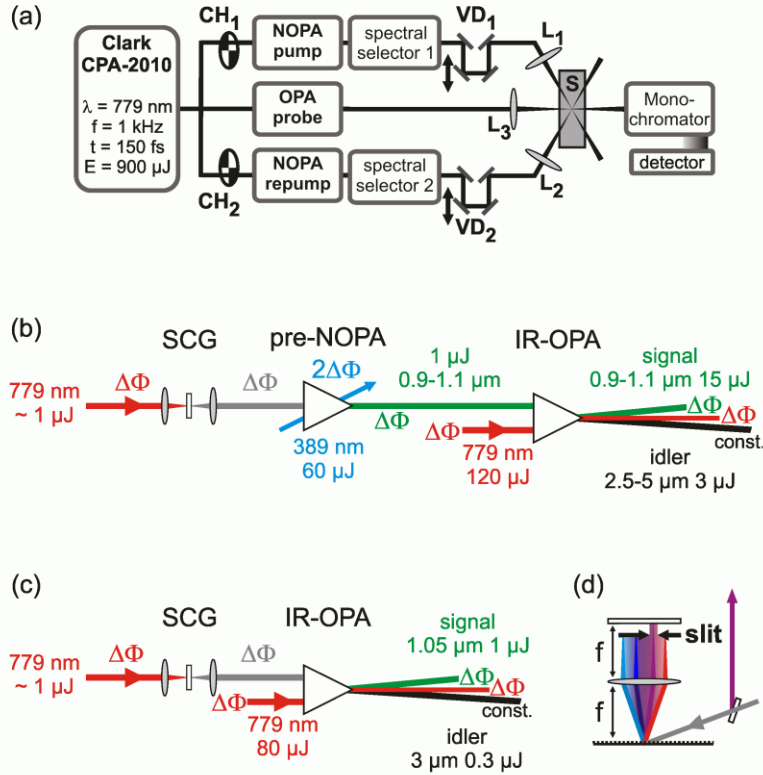


Fig. 1. (a) Schematic representation of the mid-IR pump-repump-probe setup. CH₁ and CH₂ denote chopper wheels, VD₁ and VD₂ are variable delay lines, L are lenses, and S represents the sample. (b) Setup of the hybrid NOPA used to generate the pump and repump pulses including the order of the phase fluctuations ($n\Delta\Phi$). (c) Setup of the probe OPA for the generation of the broadband probe pulses including phase fluctuations. (d) Layout of the $4f$ grating spectral selector. To avoid any spatial chirp all infrared OPAs are operated collinearly. The different pulses are shown with a slight angular separation in the figure for a better visualization.

The infrared pump pulses are sent over a motorized linear stage (M-521.DD; Physik Instrumente GmbH; variable delay VD₁ in Fig. 1) to set the delay time between pump and probe light. A hollow retroreflector with gold mirrors (50.8 mm clear aperture, 1 arcsec precision; Edmund Optics Inc.) ensures highest reflectivity and with proper alignment no spatial deviation is found when moving the delay stage over its full range of 200 mm corresponding to 1.33 ns. A mechanical chopper (CH₁) synchronized to the laser is used to obtain alternately a pumped and not pumped sample for measuring the transmission changes. The setup for the repump pulses is completely identical to the setup of the pump including the amplifier, spectral selector, chopper (CH₂), and variable delay (VD₂). To obtain adequate probe pulses we generate an infrared continuum in a 4 mm thick YAG plate and amplify the spectral region around 1.1 μm

in a single stage collinear OPA pumped by 80 μJ pulses at 779 nm. The setup is shown in Fig. 1(c). Type I amplification in a 2 mm thick LiNbO_3 crystal cut at 45° allows the generation of extremely broadband pulses around 3 μm . The pulse energy of 300 nJ allows a good signal-to-noise ratio. The broad bandwidth and the favorable dispersion properties of silicon or germanium at 3 μm can be used to compress the pulses down to the few-cycle limit. A full characterization of the pump and probe pulses will be presented in the next section. The easy wavelength tuning of the single stage OPA even allows expanding the probe range from 1 to over 5 μm in a stepwise manner. For the shorter wavelengths a BBO crystal can be used. Figures 1(b) and 1(c) additionally show the phase fluctuations of the different pulses which will be discussed in Section 3.

For polarization resolved experiments, it is important to have control over the respective polarizations of all pulses. This is achieved by broadband half-wave plates and polarizers (Thorlabs, nanoparticle linear film polarizer, 1.5 - 5 μm) for all beams. Pump, repump and probe beams are focused into the sample chamber which can be controlled in temperature and pressure. The pump beams are focused with $f = 100$ mm ZnSe lenses (L_1, L_2), the probe with a 75 mm ZnSe lens (L_3). The advantage of the ZnSe lenses compared to reflective optics is that small angles of only 10° between pump and probe beams can be experimentally realized and that no astigmatism occurs. Additionally, the high refractive index leads to less strongly curved lenses and hence reduced aberrations and an improved beam profile in the focus. The high losses due to the high refractive index can be partially compensated by anti-reflection coatings. The probe pulse is finally coupled into a spectrometer (Chromex 250is) which is set up in a Czerny-Turner configuration. The infrared light is focused into the 200 μm entrance slit via a parabolic mirror with an effective focal length of 50 mm. After an internal collimation in the spectrometer a grating with 300 lines/mm and a blaze wavelength of 4 μm is used to disperse the probe light. At the exit of the spectrometer a nitrogen cooled multichannel infrared HgCdTe detector (IR-3216; Infrared systems development Inc.) is used which offers 32 neighboring pixels with 500 μm width and 2000 μm height. The spectral resolution for one pixel is about 5 cm^{-1} (equal to 5 nm at 3 μm) which enables to cover a wavelength range of around 150 nm at once. The broadband probe pulses cover up to 1,000 nm spectral width which can be covered in a stepwise manner, simply by turning the internal grating of the spectrometer. This means that for capturing the full probe wavelength range no adjustments of the infrared amplifier have to be made. Only the grating in the spectrometer has to be adjusted to change the probe range.

The complete tunability of pump and repump in central wavelength, spectral width, and delay time allows, in combination with the extremely short and broadband probe pulses, pump-repump experiments which can reveal molecular dynamics up to the nanosecond scale with sub-100 fs time resolution and over the spectral region from 1 to 5 μm .

3. Pulse characterization

To perform ultrafast infrared pump-repump-probe experiments adequate infrared pulses must be provided. The probe pulses should cover a wide wavelength range and the pump pulses should be tunable in wavelength and spectral width for a selective excitation of the investigated systems. Our setup described in the previous section allows for the generation of such pulses. Figure 2 shows spectra of the broadband probe pulses (red) with a full width at half maximum (FWHM) of 450 nm (more than 400 cm^{-1}). The width at the 10% level is 900 nm (900 cm^{-1}) and can be employed for transient probing. The Fourier limit (calculated for zero spectral phase) of these pulses is 30 fs which corresponds to just three cycles in the mid-IR. Additionally, spectra of pump pulses with different degrees of spectral confinement (15 – 100 nm, black and blue lines) are shown in Fig. 2. The spectral width of the pump pulses can be tuned between 20 and 360 cm^{-1} .

The use of few-cycle mid-IR pulses as probe light will significantly improve the temporal resolution. To determine the pulse duration and spectral and temporal phase of our pulses we performed frequency resolved optical gating measurements based on second harmonic

generation (SHG-FROG) for both the pump and the probe light [30]. To be able to perform the SHG-FROG and to set up the f - $2f$ interferometer (to show the CEP stability, see below) with available nonlinear crystals, we slightly had to readjust the pump and probe pulses, but the obtained results can be readily transferred to the pulses used in the pump-probe spectroscopy.

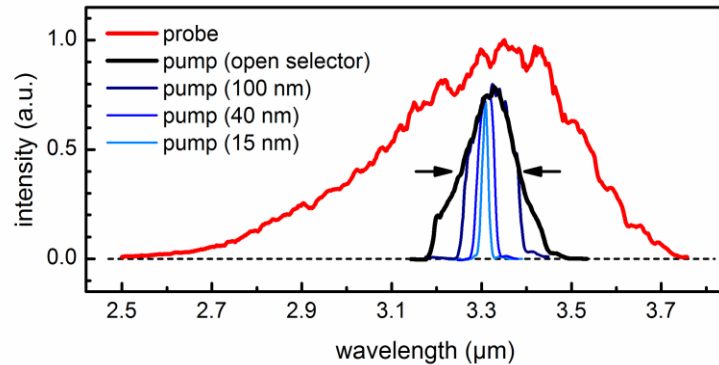


Fig. 2. Spectra of pump pulses with different spectral widths (black and blue). A typical probe pulse spectrum is shown for comparison (red).

Figure 3(a) shows the spectrum and the spectral phase of the probe pulses. The SHG-FROG measurement of the probe pulses yields a pulse duration of 45 fs which is shown in Fig. 3(b). At a central wavelength of 3.15 μm this corresponds to 4.5-cycle pulses. We used germanium plates with different thicknesses to compress the pulses and a 500 μm plate was found to be optimum [13]. The flat phase shows that this straight forward compression is sufficient and no extensive compression schemes must be applied. This is due to the fact that the second and third order chirp accumulated in the visible and near-infrared is flipped because of the use of the idler and then can be compensated by passing through transparent infrared material which has analog dispersion properties as the material in the visible and near-infrared. This increases the energy available at the sample and the stability of the setup. The time-bandwidth product for the probe pulses is 0.55, showing their excellent compression.

The spectrum and spectral phase of typical pump pulses measured without passing the spectral selector are shown in Fig. 3(c). The almost flat spectral and temporal phase (see Fig. 3(d)) shows that the pulses are close to the Fourier limit of 40 fs. The pulse duration of the pump pulse is 51 fs and the time-bandwidth product is 0.52. There is a slight post pedestal which is on the 5% level and also only contains 5% of the pulse energy. When reducing the spectral width with the spectral selector the time-bandwidth product remains nearly the same leading to an increased pulse duration of up to 850 fs for a spectral width of 20 cm^{-1} .

Another pulse property of high interest is the carrier envelope phase (CEP) [31]. In commonly used setups the infrared pulses are generated via difference frequency mixing between signal and idler from a collinear infrared amplifier. Since the pump laser for this infrared amplifier typically does not have a stable CEP, it is not manageable to obtain equal phase fluctuations of signal and idler pulses. Thus, the infrared output of the difference frequency mixing does not have a stable CEP. Since pump and probe pulses in these setups have pulse durations which lead to many cycles of the electric field this is usually of no concern. Nevertheless, if these pulses would be few cycle pulses, the phase fluctuations would lead to strong variations in the strength of the maximum electric field. And this can affect the experimental response of the investigated system although the nominal pulse energy shows very low fluctuations from pulse to pulse. Therefore a stable CEP is desired when operating with few cycle pulses to ensure a reproducible answer of the studied molecules.

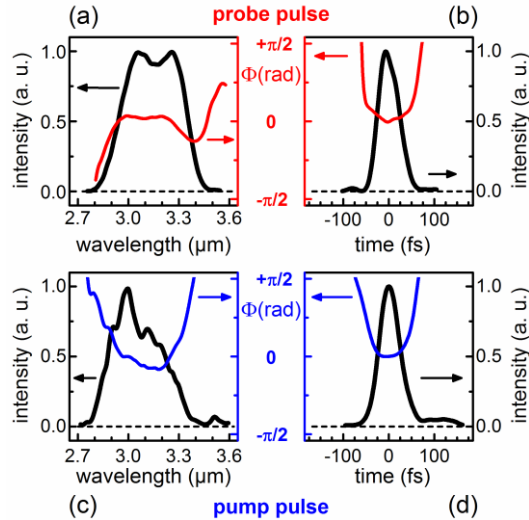


Fig. 3. Spectral intensity with corresponding spectral phase for typical probe (a) and pump (c) pulses. Temporal intensity profile and respective phase of the probe (b) and the pump (d) pulses obtained from SHG-FROG measurements.

In our setup the pump and probe pulses are few cycle pulses and have a stable CEP. This is ensured by the pulse generation setup, although our Ti:sapphire based laser system does not have a stable CEP. In Figs. 1(b) and 1(c) the order of the phase fluctuations for all participating pulses is indicated. The probe pulses are the idler output of a collinear infrared OPA. The seed for this amplifier is generated with the laser light by continuum generation in bulk which does not alter the phase fluctuations and therefore the seed has the same phase fluctuations as the laser light ($\Delta\Phi$). Since the amplifier is also pumped by the laser light with its phase fluctuations of $\Delta\Phi$, the idler pulses have a constant CEP [32]. This is due to the fact that the idler pulses inherit the relative phase difference between signal and pump pulses (besides a constant phase term).

The situation is more complex for the generation of the pump pulses due to the pre-amplifier. There the seed light is a bulk continuum generated with the laser light and therefore it has again the same fluctuations as the laser light ($\Delta\Phi$). The pre-amplifier is pumped by the second harmonic light which has twice the fluctuations of the laser light ($2\Delta\Phi$). This means that the signal pulses of the pre-amplifier have the same phase fluctuations as the seed light and hence the laser light ($\Delta\Phi$) because parametric amplification only adds a constant phase term and does not alter the fluctuations. Furthermore, the idler pulses have the same phase fluctuations ($\Delta\Phi$) because they inherit the phase difference between signal and pump phase fluctuations besides some constant phase terms ($2\Delta\Phi - \Delta\Phi = \Delta\Phi$). The infrared amplifier is pumped by the laser light ($\Delta\Phi$) and since the seed light for this infrared amplifier has the same phase fluctuations ($\Delta\Phi$) the idler pulses are again CEP stable.

To prove the phase stability we set up an f - $2f$ interferometer [31] and measured the CEP for both pulses. The setup for the interferometer is shown in Fig. 4(b). We first generate a super continuum in a 4 mm YAG with either the probe or the pump pulses. These continua range down to 500 nm. We frequency double the 1,000 to 2,000 nm part in a thin BBO crystal (SHG) and overlap it with the 500 to 1,000 nm part. The interference pattern is recorded with a fiber coupled spectrometer (HR2000 + ; Ocean Optics). Since the frequency doubled light and the original continuum have different phase fluctuations ($2\Delta\Phi$ and $\Delta\Phi$) a stable interference pattern will only appear if there are vanishing phase fluctuations. This means that the infrared pulses have a stable CEP. Figure 4(a) shows interference patterns between 500 and 900 nm for the pump pulses over three hours. The Fourier transform of the individual spectra enables the

readout of the spectral phase of the pump pulses. The resulting carrier envelope phase of the pump pulses are shown in Fig. 4(d) for the first 90 min (blue line). To show the tunability of the CEP we inserted a 4 mm ZnSe plate after 10 min, removed it after 20 min, and reinserted it after 30 min (light blue line). The standard deviation of the CEP fluctuations is 67 mrad.

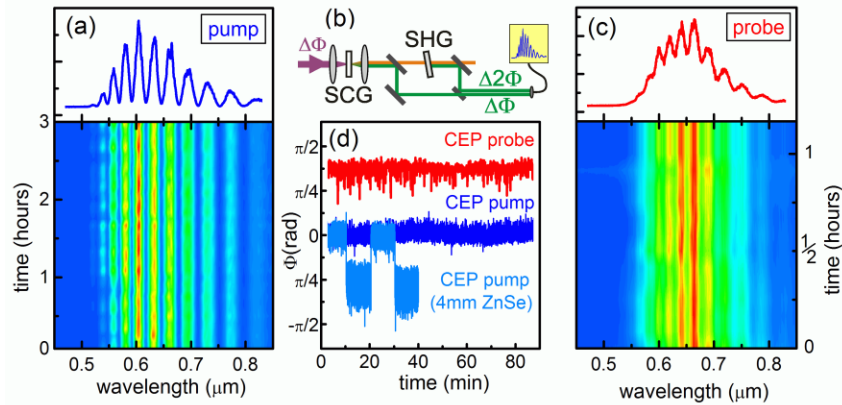


Fig. 4. Spectrum of the long time stable interference pattern from the f - $2f$ interferometer obtained with the pump (a) and probe (c) pulses. (b) Setup of the continuum generation and second harmonic based f - $2f$ interferometer. (d) Temporal evolution of the CEP of the pump (blue) and probe (red) pulses over 90 min. To demonstrate the CEP control we inserted, removed, and reinserted a 4 mm ZnSe plate after 10, 20, and 30 min (light blue).

Figure 4(c) shows the interference pattern obtained from the probe pulses which was measured over 1.2 hours. The corresponding phase is shown in Fig. 4(d) (red line). For clarity we shifted the CEP of the probe pulse upward. The standard deviation of the CEP of the probe pulses is 97 mrad. The intensity fluctuations of the interference pattern which can be observed in Fig. 4(c) are due to the continuum generation. The energy of the probe pulses is just above the threshold for proper and stable continuum generation. However, long time laser power drifts will lead to temporally unstable white light which explains the observed intensity fluctuations.

Summarizing, we have shown that broadband probe pulses and bandwidth and wavelength tunable pump pulses can be generated on the multi-100 nJ or even μ J level with our simplified setup. The pulse duration of both pulses is very close to the Fourier limit. The utilization of few-cycle IR pump and probe pulses significantly improves the time resolution. Also the carrier envelope phase of both pulses is stable. This ensures the same electric field for all measurement points. After the full characterization of the infrared (re-)pump and probe pulses we next show the potential of the setup by investigating the ultrafast dynamics of isotopically diluted lithium nitrate trihydrate and ice.

4. Validation of the temporal resolution, high sensitivity and the repump capability in $\text{LiNO}_3 \cdot (\text{HDO} + 2\text{D}_2\text{O})$ and ice

Aqueous salt hydrates serve as a promising model system for confined water molecules in a very well-defined geometrical arrangement [8,33]. In this study we document our improved measurements of isotopically diluted (5 M HDO in D_2O) aqueous lithium nitrate trihydrate. The polarization resolved FTIR spectra in Fig. 5(a) show three different features arising from three different kinds of H bonds, a strong (3385 cm^{-1}), a weak (3536 cm^{-1}) and a bifurcated one (3475 cm^{-1}), leading to parallel and perpendicular signals. This behavior is due to the crystal structure of $\text{LiNO}_3 \cdot x(\text{HDO} + 2\text{D}_2\text{O})$ with all of its OH groups lying in two mutually normal planes [8]. We performed time resolved measurements at 220 K with the new spectrometer. Figure 5(b) shows the transient change in optical density, measured at various delays after pumping of the OH group engaged in the weak H bond. For short times the ground state is

depleted by the pump pulse, leading to the ground state bleaching (GSB) at 3536 cm^{-1} . Due to the anharmonicity of the OH stretching mode an excited state absorption (ESA) is observed at 3325 cm^{-1} . Both features decay within the first 10 ps. The spectral lineaments remaining after 15 ps are assigned to transient heating of the sample. By fitting Lorentzian distributions to the transient data we achieve a FWHM of $62 \pm 10\text{ cm}^{-1}$ for the ESA which is significantly larger than that of the GSB ($20 \pm 10\text{ cm}^{-1}$). The analysis of the spectra corresponding to strong and bifurcated H bond shows widths of $125 \pm 10\text{ cm}^{-1}$ and $110 \pm 10\text{ cm}^{-1}$ for the ESAs (centered at 3140 cm^{-1} and 3260 cm^{-1}) and $30 \pm 10\text{ cm}^{-1}$ and $80 \pm 10\text{ cm}^{-1}$ for the GSBs [8].

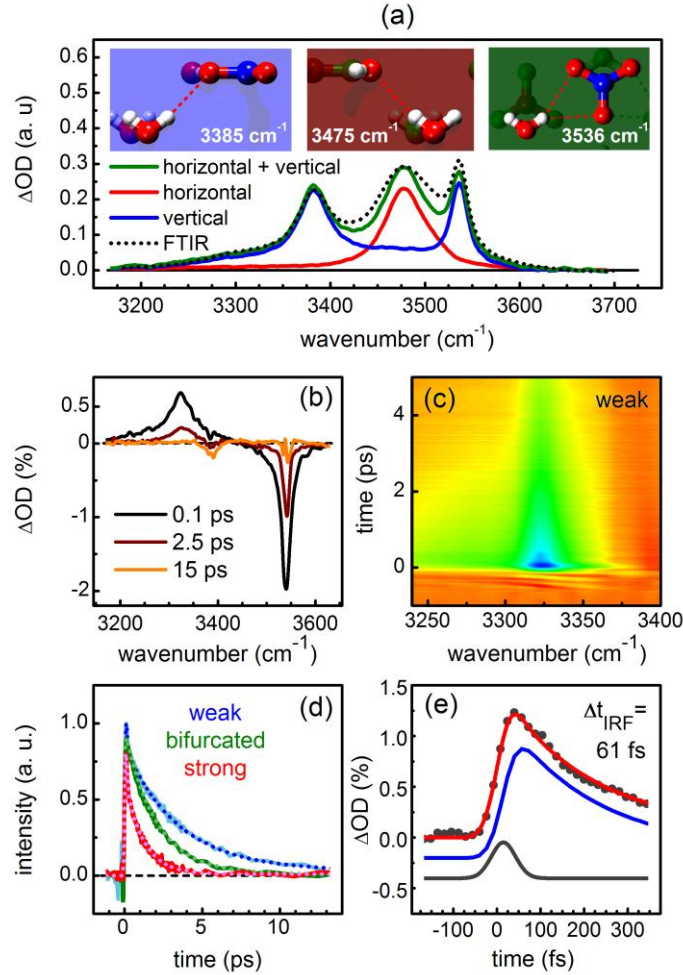


Fig. 5. (a) FTIR spectra of the OH stretching region of the sample. It can be seen how the three resonances are polarization separated due to the orthorhombic structure of the crystal. The corresponding H bonds are depicted in the insets above the spectrum. (b) Transient spectra after excitation of the OH group engaged in the weak H bond. The delay times between pump and probe are 0.1 ps (black), 2.5 ps (brown), and 15 ps (orange). (c) Transient measurement of the weak OH stretching resonance for one detector position. (d) Transient signal of the maximum of the excited state absorption of the weak (blue), bifurcated (green), and strong (red) OH stretching resonances in $\text{LiNO}_3 \times (\text{HDO} + 2\text{D}_2\text{O})$ including fits. (e) Transient signal over the first few hundred femtoseconds of an ice sample to demonstrate the ultrafast instrumental response function of 61 fs.

Figure 5(d) shows the temporal evolution of the ESA after excitation of the three individual OH stretching vibrations at the center wavelength of the associated GSB. After a short time of

about 0.3 ps all three signals start to decay exponentially. The fast dynamics observed around delay time zero may be influenced by coherent artifacts that become more significant in the blue shifted part of the ESA approaching the excitation wavelength of the pump beam. The extracted lifetimes for strong, bifurcated and weak H bond are 1.1 ± 0.1 ps, 1.9 ± 0.2 ps and 3.4 ± 0.3 ps. It is noteworthy that the lifetime, just like the strength of the observed H bonds, correlates not only with the red shift of the respective OH stretching, but also with the magnitude of their anharmonicity, indicated by the spectral shift between GSB and ESA. The lifetimes in $\text{LiNO}_3 \times (\text{HDO} + 2\text{D}_2\text{O})$ are considerably faster than those of isolated HDO monomers that are on the order of 6.8 ps [33–35] and exceed those measured in isotopically diluted ice Ih of about 380 fs [36]. To show the spectral coverage of the 32 pixel detection, Fig. 5(c) presents the transient measurement from 3240 to 3400 cm^{-1} of the weak OH stretching resonance. The entire transient spectrum shown in Fig. 5(b) is obtained by adding the transient measurements from other spectral regions. For this purpose no optical alignment is needed. Just the internal grating of the detection setup has to be rotated.

A first estimation of the temporal resolution is obtained from the FROG measurements of the pump and probe pulses. The FWHM of the convolution between both pulses is 72 fs. Although a possible resolution of 72 fs is already quite competitive, it has to be considered that pump and probe pulses were slightly optimized to perform the FROG and CEP measurements. A better method to determine the temporal resolution of our new spectrometer is the analysis of the transient signals. This is superior to a pure optical determination by cross correlation in a nonlinear crystal as it incorporates not only the pulse durations, but also any possible broadening mechanisms in the interaction region. Furthermore it measures the instrumental response function directly at the sample position. In addition, no restraints as continuum generation for the CEP measurements must be regarded.

The instrumental response function was determined by the increase of the ESA (at 2920 cm^{-1}) in pure H_2O ice excited in the maximum of the OH stretching mode at 3300 cm^{-1} . As shown in Fig. 5(e), we find a time resolution of 61 fs. To fit the experimental trace (dark grey solid circles, red curve for the fit) we included a coherent artifact (grey curve) in addition to the exponentially decaying molecular response (blue curve). The coherent artifact steepens the initial rise and slightly shifts the apparent time zero. If we do not include the artifact in the fit, an even better time resolution would be concluded. The future full analysis will clarify this situation. We can, however, be sure from both the pulse convolution and the spectroscopic measurement that the new spectrometer has a temporal resolution far better than 100 fs.

Extracting the pulse durations from the cross correlation represented by the increase of the measured signal yields time bandwidth products of 0.6 ± 0.1 , which are in good accordance with the FROG measurements shown in Section 3. The setup allows to determine transmission changes with just a strength of $1.5 \cdot 10^{-4}$ for short measurement times which corresponds to $6 \cdot 10^{-5}$ OD. The extracted lifetimes are in good agreement with our former measurements that rendered lifetimes of 1.2 ± 0.3 ps, 1.7 ± 0.3 ps and 2.2 ± 0.3 ps for the strong, bifurcated and weak H bond [8]. The deviation of about 1 ps for the weak bond is believed to be a result of an improved fit procedure which explicitly considers the coherent artifact. The artifact is most distinctive in the signal from the OH group engaged in the weak H bond because of the smaller red shift of the ESA. On the other hand the observation in the new recording may be due to the improved signal-to-noise ratio. The extremely high temporal resolution and excellent sensitivity of the setup should be noted. The employed pump pulse energy was just 1 μJ , to avoid artifacts due to excessive heating of the sample. Even this comparatively low excitation energy already results in about 10% excitation of the sample. The signal-to-noise ratio of the measurements is extremely satisfactory. The probe pulses have energies on the order of 100 nJ.

To prove the repump capability of our setup, we performed pump-repump-probe measurements in a 5M HDO in H_2O sample at a temperature of 230 K. The sample thickness was 10 μm , the absorption spectrum of the sample is shown in the lower right hand part of Fig. 6 (black curve, note differing scaling). Due to the low concentration of OD oscillators as

compared to the OH oscillators, the OD stretch band at 2440 cm^{-1} is much weaker than the OH stretch at 3250 cm^{-1} . When we raise the temperature of the sample by 20 K a shifted spectrum is found [37]. The difference between the two spectra is shown as dotted blue line. Since the deposition of energy into one of the high lying stretching modes yields a heating of the sample after the relaxation of the high frequency modes, this difference spectrum represents the transient response at long delay times [37]. Thus, we expect a build-up of the GSB with the instrumental response function, and a subsequent relaxation to a constant signal value, which depends on the probed spectral position and can be deduced from the stationary difference spectrum.

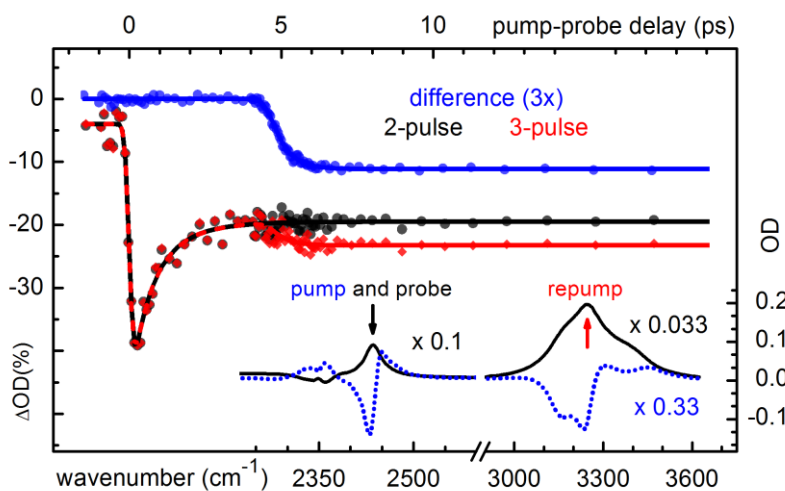


Fig. 6. Transient 2-pulse (black), 3-pulse (blue) and difference signal (red) measured at 2440 cm^{-1} (OD stretching mode) in a 5M HDO in H_2O sample at 230 K. The solid lines are fits according to a simple exponential model as guide to the eye. The symbols represent the raw data. The delay between pump and repump pulse is set to 4.5 ps. At this time the pump-repump-probe curve shows an additional signal due to further heating induced by the repump pulse absorbed by the OH stretching modes. The inset shows the absorption spectrum of the sample (black, note differing scaling factors) and the difference spectrum obtained by heating the sample by 20 K (blue dotted). The spectral position of pump, repump and probe pulse at the OD and OH stretch band are shown as black and red arrows.

For the pump-repump-probe measurements the pump and probe beams were tuned in resonance with the fundamental OD stretching vibration at 2440 cm^{-1} (4100 nm). The repump beam was set to 3250 cm^{-1} (3075 nm), corresponding to the equivalent excitation in the OH regime. The black curve in Fig. 6 shows the pump induced signal. It consists of a ground state bleaching of the OD stretching vibration around zero delay time (sub-100 fs rise). The aforementioned long-term signal is due to a spectral shift of the OD stretching band caused by heating of the sample [37]. An effective signal decay of 1.1 ps is determined from the measurement and sets a lower limit for the heating time. The initial change of optical density is 35%, a very large value for MIR experiments. This shows that the 3 μJ pump energy together with the 100 μm focal diameter in the sample is well sufficient for any transient measurements on water or ice. At 4.5 ps after the pump pulse the repump pulse is applied. The excitation of the OH oscillators is not immediately visible in the OD stretching region, but results in an additional heating of the sample with a new rise time of 0.5 ps, in which the high-lying vibrations located on individual water molecules relax to low lying thermal modes including many molecules. This manifests itself as a clearly visible additional signal in the OD stretching vibration region and can only be observed in 3-pulse experiments.

The blue curve shows the pure repump-induced effect as a difference between the 3- and 2-pulse signal transients. The 3.5% signal increase at 4.5 ps is recorded with excellent signal-to-noise ratio. This is in striking difference to the pure signals with and without repump. From earlier work we know that the pulses of our Ti:sapphire pump system are highly correlated, i.e. subsequent pulses are nearly identical in energy despite a sub-1% overall fluctuation [38]. The repump is blocked on every other shot and thereby the high degree of correlation is optimally used to reduce the fluctuations in the difference signal just as this is done in our broadband UV/Vis spectrometer [39].

Extended 3-pulse experiments are in progress to elucidate this combined action of OD and OH induced heating of ice. The first data presented here not only show the possibility to perform three-color experiments with excellent signal-to-noise. They also demonstrate that the high spectral tunability of the setup in combination with well engineered samples facilitates the interpretation of the data. In this way the influence of overlapping pump-probe signals on top of the pump-repump-probe signal [40] can be minimized.

5. Summary and conclusions

In summary, we have presented a detailed description of a novel setup for IR pump-repump-probe spectroscopy with few-cycle, carrier-envelope phase stable pulses. A Ti:sapphire pump system operating with 1 kHz and a modest 150 fs pulse duration supplies the total pump energy of just 0.6 mJ. The pump and repump pulses are tunable in the range from 2,000 to 10,000 cm^{-1} . The range from 6,250 cm^{-1} downward is covered by the idler of the IR-OPA, the higher energy range by the signal. This enables investigations on a broad variety of vibrations (e.g., OH, NH, CH stretching modes and overtones) important for a plethora of biological and chemical systems. Pump and repump spectral widths are controlled by grating selectors. The pulses generated in this way have a spectral bandwidth between 20 and 360 cm^{-1} and are nearly Fourier limited with a time-bandwidth product of 0.55 ± 0.05 . The probe pulses are shorter than 50 fs with an unprecedented spectral width of 450 cm^{-1} (FWHM). A first estimate of the ultrafast instrumental response function as short as 60 fs has been found. This is even shorter than the fastest vibrational dynamics like the relaxation of the OH stretching mode in ice Ih [17,19,41] and will allow the full temporal resolution of these processes.

The complete experimental system, delivering some of the shortest pulses applied for IR spectroscopy to date [12–14,42,43], allows to determine transient absorption changes smaller than 10^{-4} OD. This high sensitivity allows for measurements with extremely low pump intensities, to suppress artifacts due to strong temperature jumps [37]. The shot-to-shot stability of the presented setup is exceptionally high, allowing for high quality measurements with moderate measurement time. A typical time-resolved measurement like the one shown in Fig. 5(c) consists of about 130 time delays and takes around 45 minutes. The transient spectra presented in Fig. 5(b) were recorded by one selected pixel of the IR detector via turning the grating of the spectrometer and each was recorded in only 20 minutes. In the future we will implement and validate a procedure that uses all 32 pixels in parallel and should decrease the recording time by more than an order of magnitude.

With the available pump pulses, we have shown measurements with 8.5% of the molecules in the $\text{LiNO}_3\text{x}(\text{HDO} + 2\text{D}_2\text{O})$ sample volume excited. For a thin ice sample even more than half of the OH stretch absorption is bleached. This allows the ready performance of pump-repump-probe measurements with large reasonable signal strength and excellent signal-to-noise. In combination with the extremely high time resolution, re-excitations within the short time window spanned by the lifetime of the initially excited vibrations are possible without temporal overlap of pump and repump pulses. Thus, we can avoid artifacts caused by the temporal overlap between pump and repump pulses. Excitations to higher lying levels will not only enable us to investigate the properties of higher lying vibrational states, but might also serve as a pathway to optically induced chemical reactions like proton transfer initiated by mid-IR pulses, which has not yet been achieved.

The warming up of the system and the fine adjustment of the setup on a day-to-day basis only takes around two hours. The alignment of the invisible mid-IR pulses is greatly alleviated by the fact, that all IR-OPA stages are collinear. Thus, the visible components of the NOPA output can be employed as alignment guides. The low time consumption of both daily alignments and data recording makes the setup very suitable for the investigation of biological, short-lived samples, and enables high data output under routine operation. Finally, it is possible to tune the pump and repump pulses to the visible and UV via minor modifications of the NOPA layouts. This will allow us to carry out UV-pump-IR-probe experiments that can for example provide important information on the mechanisms of UV induced DNA damage or photosynthesis.

Acknowledgments

Financial support of this work by Deutsche Forschungsgemeinschaft through the excellence cluster 'Munich Center for Advanced Photonics' (MAP) and the SFB 749 is gratefully acknowledged.